Received: 13 October 2021 | Revised: 27 January 2022 | Accepted: 29 January 2022

DOI: 10.1111/hepr.13754

ORIGINAL ARTICLE

Hepatology Research

Perturbation of Wnt/β-catenin signaling and sexual dimorphism in non-alcoholic fatty liver disease

Matthew M Yeh[1] | Xiuhui Shi[2] | Jingxuan Yang[2] | Min Li[2] | Kar-Ming Fung[3] | Sayed S. Daoud[4]

[1]Department of Laboratory Medicine and Pathology, University of Washington, School of Medicine, Seattle, Washington, USA

[2]Department of Medicine and Department of Surgery, The University of Oklahoma Health Sciences Center, Oklahoma City, Oklahoma, USA

[3]Department of Pathology and Stephenson Cancer Center, University of Oklahoma Health Sciences Center, Oklahoma City, Oklahoma, USA

[4]Department of Pharmaceutical Sciences, Washington State University Health Sciences, Spokane, Washington, USA

Correspondence

Sayed S. Daoud, Department of Pharmaceutical Sciences, Washington State University Health Sciences, 415 PBS, Spokane, WA 99202, USA.
Email: daoud@wsu.edu

Funding information

CPPS-WSU, Grant/Award Number: 17A-2957-9838

Abstract

Aims: The prevalence of non-alcoholic fatty liver disease (NAFLD) and its progression to non-alcoholic steatohepatitis (NASH) is higher in postmenopausal women than men. The aim of this study was to determine the molecular mechanisms underlying this sexual dimorphism in NAFLD.

Methods: A total of 24 frozen liver samples of both sexes (normal and NAFLD/NASH) were used in this study. Total RNAseq was first used to identify differentially expressed genes (DEGs) between samples. Enrichment analysis of Gene Ontology (GO), Kyoto Encyclopedia of Genes and Genomes (KEGG), and Reactome were used to analyze biological pathways. RT^2 profiler polymerase chain reaction (PCR) arrays were used to identify genes associated with the biological pathways. Immunoblotting was used to validate protein expression of certain genes.

Results: We identified 4362 genes that are differentially expressed between NAFLD/NASH and normal samples; of those 745 genes were characterized as sex specific in NAFLD/NASH. Multiple pathway analysis platforms showed that Wnt-signaling is a candidate shared for a common biological pathway-associated with NAFLD/NASH. Using Wnt pathway focused PCR array we identified many genes involved in canonical pathway (Wnt/β-catenin activation) such as *CTNNB1*, c-*Myc* and *CCND2* are overexpressed in female cases, whereas these genes are either not detected or downregulated in male cases. Immunoblot analysis validated the expression of CTNNB1 in female cases but not in male protein samples.

Conclusions: Our study suggests, for the first time, that the activation of canonical Wnt signaling could be one of the main pathways associated with sexual dimorphism in NAFLD and NASH.

KEYWORDS

non-alcoholic fatty liver disease, non-alcoholic steatohepatitis, RNA-seq, RT^2-profiler PCR arrays, sexual dimorphism, Wnt/β-catenin

Abbreviations: NAFLD, non-alcoholic fatty liver disease; NASH, non-alcoholic steatohepatitis; RNA-seq, RNA sequencing; RT^2-PCR Array, quantitative RT-PCR array; PCA, Principal Component Analysis; WB, Western blot; DEGs, differentially expressed genes; GO, Gene Ontology; KEGG, Kyoto Encyclopedia of Genes and Genomes; CTNNB1, β-catenin; CCND2, cyclin D2; SNP, single nucleotide polymorphism; HCC, hepatocellular carcinoma.

INTRODUCTION

Non-alcoholic fatty liver disease (NAFLD) is the leading cause of chronic liver disease that affects 25% of the US population.[1,2] NAFLD is commonly associated with obesity, diabetes, and metabolic syndrome, but it could affect non-obese individuals as well.

The disease spectrum ranges from bland steatosis with or without inflammation (non-alcoholic fatty liver, NAFL) to steatosis with inflammation and hepatocellular injury (non-alcoholic steatohepatitis, NASH), fibrosis, cirrhosis, and hepatocellular carcinoma (HCC).[3] Because of lack of reliable noninvasive predictable biomarkers, the diagnosis of NASH is mainly limited to histopathological evaluation of liver samples defined by liver biopsy-proven hepatocellular steatosis, lobular inflammation, and evidence of hepatocyte injury such as ballooning degeneration.[4] Recent progress in "omics" research has allowed for further identification of various genetic alterations in NAFLD disease progression. For example, the single nucleotide polymorphism causing a substitution of isoleucine to methionine at position 148 in patatin-like phospholipase domain-containing 3 (*PNPLA3*, rs738409) was identified to be the most predictive variant associated with NAFLD.[5] PNPLA3 has hydrolytic activity toward triacylglycerols, diacylglycerol and monoacylglycerol. The I148M substitution causes loss of function in the enzyme, associated with higher liver lipid content, greater NASH activity, and increased risk of liver fibrosis and development of HCC.[6] Other widely investigated genetic variants include transmembrane 6 superfamily membrane 2 (*TM6SF2*) rs58542926C > T, membrane bound o-acyltransferase domain-containing 7 (*MBOAT7*, rs641738C > T), and glucokinase regulator (*GCKR*, P446L). Similarly, these variants are also associated with increased NAFLD severity and risk of fibrosis.[7–9]

The increased risk of central obesity and subsequent diabetes in some racial/ethnic minority populations confers additional risk for the development of advanced fibrosis and cirrhosis in NAFLD disease progression. A meta-analysis of US population-based studies reported the highest prevalence of NAFLD is in Hispanic population as compared to Non-Hispanic Caucasians or African Americans.[1] Likewise, many studies have also showed that there are gender disparities in NAFLD with respect to disease severity, fibrosis, and NASH.[10] The prevalence and severity of NAFLD are shown to be higher in men than in women during the reproductive age, whereas after menopause, NAFLD occurs at a higher rate in women, especially after 50 years suggesting the protective role of estrogen.[11–13] These data suggest that a better understanding of the interplay among menopausal status, metabolic comorbidities, and sex steroids in NAFLD pathogenesis is needed to develop better clinical management of the disease. Further, the molecular mechanisms underlying gender disparities in NALFLD risk remain incompletely understood. Without such information, the promise of developing effective clinical management and treatment of NAFLD based on gender or racial/ethnic disparities will likely remain limited. Therefore, in the current study, we apply whole RNA sequencing (RNA-seq) coupled with pathway-focused polymerase chain reaction (PCR) profiling using RT^2 Profile PCR Array System of frozen liver tissue samples (normal and NAFLD/NASH) of both sexes to uncover the transcriptome signature and molecular pathways potentially associated with the observed sexual dimorphism in NAFLD, thereby providing an opportunity for tailored approach and better clinical care management of NAFLD.

METHODS

Ethics statement

The Institutional Review Board (IRB) at Washington State University (WSU) approved the protocol of the current study. Twenty-four snapped frozen tissue samples (eight included in original RNA-seq analysis and sixteen for pathway-focused PCR profiling and immunoblotting) were obtained from the IRB approved University of Minnesota—Liver Tissue Cell Distribution System. All specimens with anonymized identifiers were histopathological confirmed by a pathologist.

RNA extraction and whole-transcriptome sequencing (RNA-seq)

Total RNA was extracted from eight frozen liver biopsy specimens (four normal and four NAFLD/NASH) of both sexes using the RNeasy Mini Kit (QIAGEN). RNA concentration was measured with NanoDrop (Thermo Fisher Scientific). Extracted RNA with RNA Integrity Number (RIN) > 7 was shipped frozen to QuickBiology (Pasadena, CA) for cDNA library preparation according to KAPA Standard mRNA-Seq polyAselected kit with 201–300 bp KAPA Biosystems, using input of 250 ng total RNA. The final library quantity and quality was checked by Agilent 2100 Bioanalyzer and Qubit 2.0 Fluorometer (Life Technologies). The generated 30 million paired end reads of 150 bp RNA was sequenced on the Illumina HiSeq 4000. A data quality check was done on Illumina SAV. Demultiplexing was performed with Illumina Bcl2fastq2 v2.17 program.

RNA sequencing analysis

The reads were first mapped to the latest UCSC transcript set using Bowtie2 version 2.1.0.[14] and the gene expression level was estimated using RSEM v1.2.15.[15] Differentially expressed genes were identified using edgeR program.[16] Genes showing altered expression with $p < 0.05$ and more than 1.5-fold changes were considered differentially expressed. Goseq was used to perform the Gene Ontology (GO) enrichment analysis[17] and Kobas was used to perform pathway analysis.[18] Associated Kyoto Encyclopedia of Genes and Genomes (KEGG)[19] signaling pathways were analyzed using the Bioconductor package ROntotools.[20]

WNT signaling pathway RT^2 profiler PCR array

WNT pathway-focused PCR array (QIAGEN PAHS-043Y) which measure mRNA levels of 84 genes involved in WNT signaling or

targets of the WNT pathway was used to confirm RNA-seq results of the GO enrichment analysis. Total RNA was isolated from eight frozen liver biopsy specimens (four normal and four NAFLD/NASH) of both sexes using the RNeasy Mini Kit (QIAGEN) as described above. The cDNA was prepared from 2 μg of total isolated RNA by using the RT^2 PCR array first strand kit in accordance with the manufacturer's protocol (QIAGEN). The synthesized cDNA was mixed with the RT master mix (RT^2 SYBR Green; QIAGEN; Cat. No. 330529) in accordance with the supplier's instructions and pipetted into the 96-well PCR array plates. The array reactions were performed by using an Applied Biosystems (ABI) 7500 real-time-polymerase chain reaction system (ABI) in accordance with the manufacturer's instructions (QIAGEN) under the following conditions: 95°C for 10 min, then 40 cycles at 95°C for 15 s and 60°C for 1 min. Each array contained five separate housekeeping genes (HKG) (*ACTB*, *GAPDH*, *HPRT1*, *B2M* and *RPLP0*) that are used for normalization of the sample data. In addition, each array contains a panel of proprietary controls to monitor genomic DNA contamination (GDC) as well as the first strand synthesis (RTC) and real-time PCR efficiency (PPC). All data from the PCR was collected and uploaded onto the data analysis web portal at http://www.qiagen.com/geneglobe.

Data analysis of PCR array

Normalization of the sample data was performed by calculating the ΔCt for each gene of interest (GOI) in the plate (Ct value of GOI-Ct value of HKG) followed by ΔΔ calculations (ΔCt (Test Group; NAFLD/NASH)−ΔCt (Control Group; Normal)). The Fold Change is then calculated using 2^(−ΔΔCt) formula.[21] The data analysis web portal also plots scatter plot, volcano plot, clustergram and heatmap.

Statistical analysis of PCR array data

The RT^2 Profiler PCR Array web portal does not perform any statistical analysis beyond calculation of the *p*-values using a Student's *t*-test based on the triplicate 2^(−ΔCt) values for each gene in the Test Group (NASH) compared to the Control Group (Normal). Previous reports by the Microarray Quality Control (MAQC) and others have shown that a ranked list of genes based on fold-change and *p*-value calculation was sufficient to demonstrate reproducible results across multiple microarray and PCR Arrays including the RT^2 Profiler PCR Arrays.[22,23]

Western blot analysis

The Western blot analysis was performed as previously described with modifications.[24] In brief, protein samples from eight frozen liver tissue lysates (four normal and four NAFLD/NASH) of both sexes (different cohorts were denatured and loaded onto NuPAGE™ 4%–12% Bis-Tris gels). After electrophoresis, proteins were transferred to Odyssey® nitrocellulose membranes (LI-COR Biosciences). Membranes were blocked for 2 h with TBST Buffer (TBS-containing 0.1% Tween 20 + 5% Bovine serum albumin) then incubated for overnight with primary antibodies diluted in TBST Buffer. The human beta-catenin (#138400), PITX2 (PA598817), FRZB (PA5104120) and WIF1 (PA512299) antibodies were purchased from Thermo Fisher Scientific. After incubation with primary antibodies, the membranes were washed with TBST Buffer three times. Then the membranes were incubated for 1 h with IRDye800CW-conjugated goat antirabbit IgG and IRDye680-conjugated goat anti-mouse IgG secondary antibodies (LI-COR Biosciences) diluted in Odyssey Blocking Buffer. The blots were then washed three times with TBST Buffer. Proteins were visualized by scanning the membrane on an Odyssey® FC Infrared Imaging System (LI-COR Biosciences) with both 700- and 800-nm channels.

RESULTS

Clinical characteristics of the study population

A total of 24 snapped frozen liver tissue samples from White, non-Hispanic population of both sexes were used in this study (Table S1). The average age of NAFLD/NASH patients were 54 years with 40% diabetics and obese (median BMI = 35.6 kg/m^2). The average fibrosis of the two cohorts (stage F1–F3) was 2.3, mainly in NASH female samples (postmenopausal).

Clustering analysis of identified transcripts can discriminate between normal and NAFLD/NASH

To identify genes that are differentially expressed in human NAFLD, we performed RNA-seq analysis using RNAs extracted from four human NAFLD/NASH cases of both sexes (case 5 through 8) and four normal liver tissue samples (case 1 through 4). On average, 27 million and 26 million sequencing reads were obtained, respectively. More than 95% of reads were aligned to the reference genome (UCSC hg19), and more than 99% of the aligned reads were stranded. EdgeR was used to perform the differential gene analysis where we identified 4362 genes that are differentially expressed (false discovery rate (FDR) *q*-value < 0.05 and foldchange > 1.5), including genes previously identified.[25] For example, fibulin 5 (*FBLN5*), glypican 3 (*GPC3*), insulin-like growth factor-5 (*IGFBP5*), transforming growth factor, beta1 (*TGFB1*), thrombospondin 2 (*THBS2*) were markedly upregulated in NAFLD/NASH cases, whereas serum amyloid A2 (*SAA2*), acetyl-CoA acyltransferase2 (*ACAA2*) were significantly downregulated. *PNPLA2*, which is an important paralog gene of *PNPLA3* that is associated with NASH, was also significantly suppressed.[26] Detailed information on differentially expressed genes (DEGs) are presented in Table S2. Complete discrimination was seen in the hierarchical clustering heatmap comparing cases with NAFLD/NASH to normal samples (Figure 1a). Principle components analysis (PCA) of

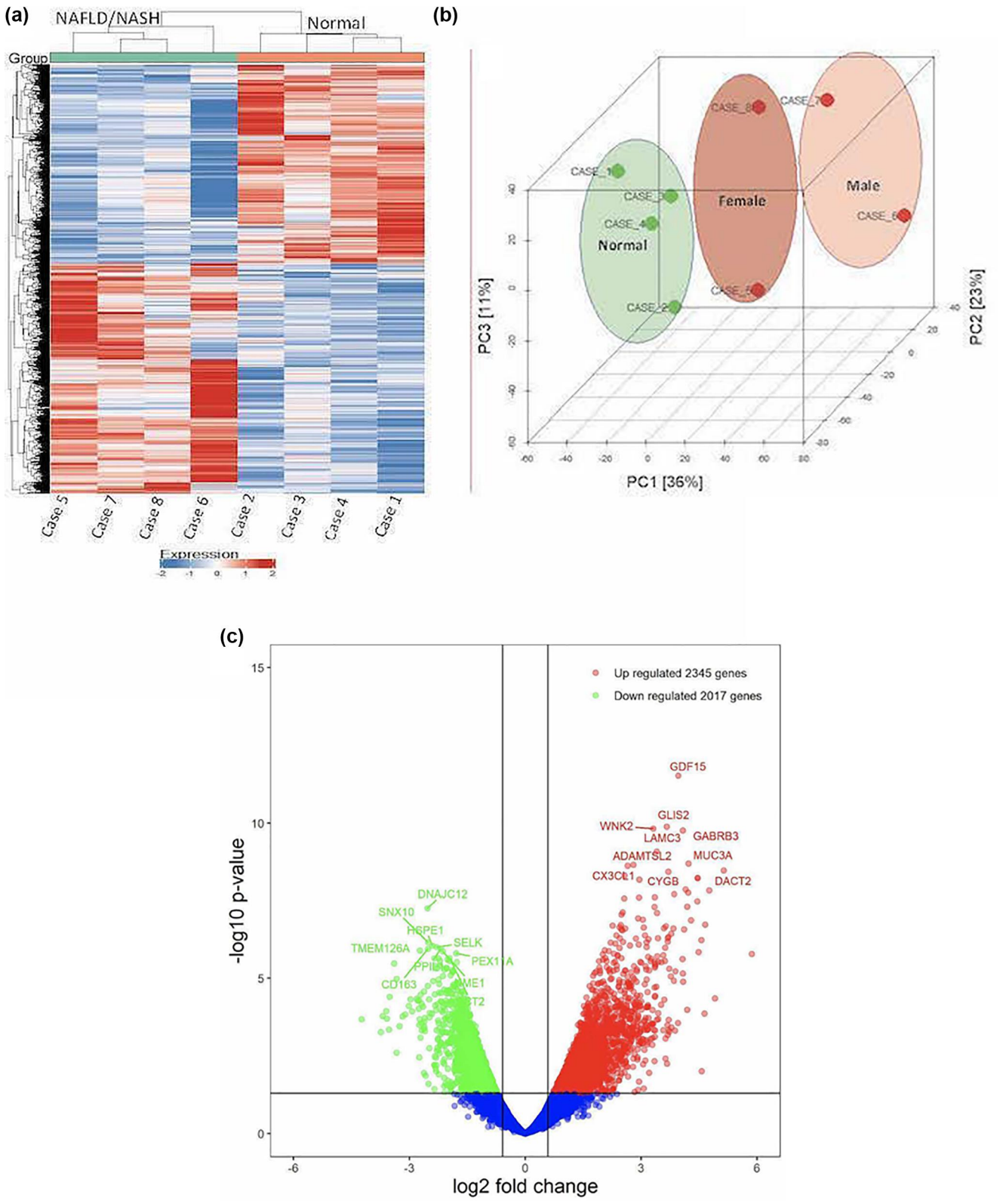

FIGURE 1 Clustering dendrogram of differentially expressed genes (DEGs) between NAFLD/NASH cases and normal subjects. (a) The heatmaps show DEGs for human NAFLD cases (case 5–8) along with normal liver tissues (case 1–4). Samples were grouped using hierarchical clustering based on similar expression profiles. Heatmap color codes for column labels are indicated on the center bottom of the heatmaps. (b) Gene expression profiling in three-dimensional space by Principal Component Analysis (PCA). The first principal component with the highest variation (36%) is shown in the *X*-axis and separates the samples based on Normal and NAFLD subjects. The normal (green), NAFLD, female (dark red), and NAFLD male (pink) samples formed three separate clusters on PCA based on disease and gender. (c) Volcano plot of DEGs in NAFLD compared to normal samples. The *x*-axis indicates the differential expression profiles, plotting the fold-induction ratios in a log−2 scale. The *y*-axis

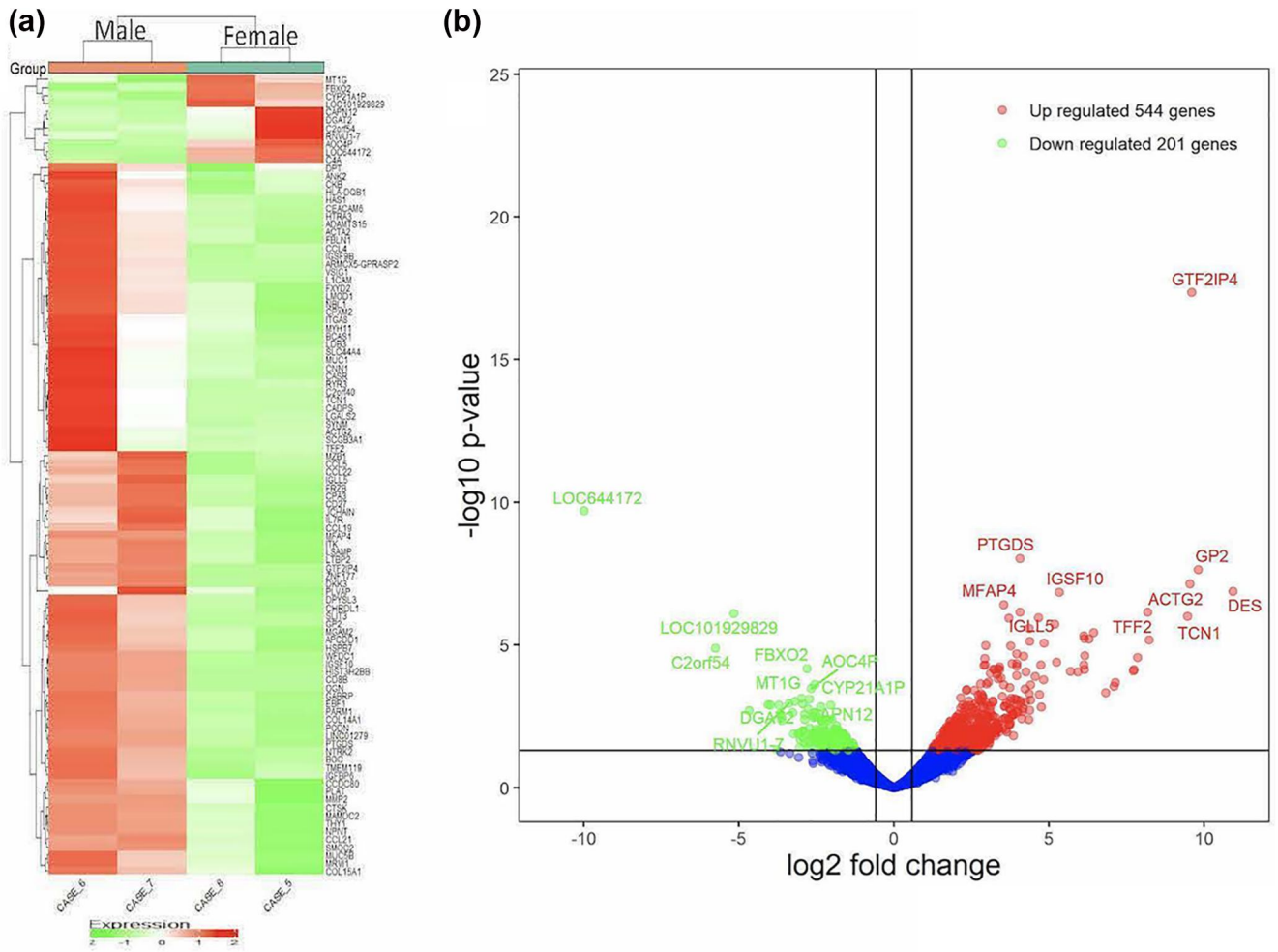

FIGURE 2 Clustering dendrogram of differentially expressed genes (DEGs) between male and female cases in NAFLD. (a) The heatmaps show differential expression of 745 genes between male and female case in NAFLD. The supervised hierarchical clustering analysis clearly distinguish between male and female cases. Red and green color indicate high and low transcripts level relative to normal based on overall gene expression. Colored bar above heatmap show female cases in green and males in red. (b) Volcano plot of 745 genes expressed between male and female cases in NAFLD. Red and green dots represent upregulated and downregulated genes, respectively, while blue represents genes that have no significant difference

DEGs demonstrated significant separation based on disease state (normal vs. NAFLD/NASH) and sex (female vs. male) along primary component (PC1) accounted for 36% of the variation between samples (Figure 1b). Volcano plot (Figure 1c) shows significance versus fold change of DEGs on the *y* and *x* axes, respectively. The top 15 significant genes are labeled. Among the highly overexpressed genes (red) are growth differentiation factor (*GDF15*) which is involved in the stress response program of cells and TGFbeta signaling; *GLIS2*, which acts as a transcriptional activation repressor mediated by β-catenin (*CTNNB1*) in the Wnt signaling pathway; *CX3CL1*, which has a chemokine activity and involved in inflammatory diseases such as NAFLD. Among downregulated genes (green) are *SELK* and *CD163*. Both are protectors of cells from oxidative stress and inflammation.

Comparison of NAFLD/NASH transcriptome profile in males and females

The identification of DEGs between male and female cases in NAFLD/NASH was of interest as these could provide leads of potentially useful explanation underlying sexual dimorphism in NAFLD/NASH disease. EdgeR was used to perform the differential gene analysis where we identified 745 genes that are differentially expressed between female and male cases (FDR q-value < 0.05 and foldchange > 1.5) as described above. Detailed information on these genes is presented in Table S3. Complete discrimination was seen in the hierarchical clustering heatmap of top 30 genes when comparing NAFLD/NASH cases in female versus male (Figure 2a). Volcano plot (Figure 2b) shows significance versus fold change of DEGs on the *y*

indicates the statistical significance of the difference in expression (p-value, t-test) in a log10 scale. Differentially expressed genes ($p < 0.05$) appear above the horizontal line. Red and green dots represent upregulated and downregulated genes, respectively, while blue represents genes that have no significant difference

and *x* axes, respectively. The top 10 significant genes are labeled. Among the highly overexpressed genes (red) in male cases (male specific genes) are Glycoprotein 2 (*GP2*) and Transcobalamin 1 (*TCN1*). Both are involved in innate immune response. Examples of genes that are downregulated (green) are Diacylglycerol o-acyltransferase 2 (*DGAT2*) which plays a major role in triglyceride (TG) synthesis; F-Box protein 2 (*FBXO2*) which mediates the ubiquitination and subsequent proteasomal degradation of target proteins; and Metallothionein 1G (*MT1G*) which is transcriptionally regulated by heavy metals & glucocorticoids and associated with HCC.

Biological pathways and specific transcripts associated with NAFLD/NASH

We then subjected the DEGs to Gene Ontology Annotation (GO analysis) to categorize these genes into relevant functions. In our study, over 50% of DEGs were grouped into 33 biological process terms, 13 cellular component terms and 4 molecular function terms, as shown in Figure 3a. Most of the enriched biological process terms of the DEGs were categorized into metabolic processes. Most significant pathway associated with the biological process terms was shown to be involved in "regulation of Wnt signaling" (GO:0030111). The full list of GO enrichment analysis data is provided in Table S4.

To further study additional relevant biological pathways, KEGG pathway analysis was also performed based on the annotation results. The top 15 KEGG pathways among the up- or down-regulated DEGs is shown in Figure 3b. Among the top KEGG enriched pathway was "NAFLD" (hsa04932), as well as pathways associated with Prion, Alzheimer, Huntington, and Parkinson diseases. The full list of KEGG Pathway enrichment analysis data is provided in Table S5. Next, we performed pathway-based analysis in Reactome to identify possible shared pathways between the three platforms: GO, KEGG and

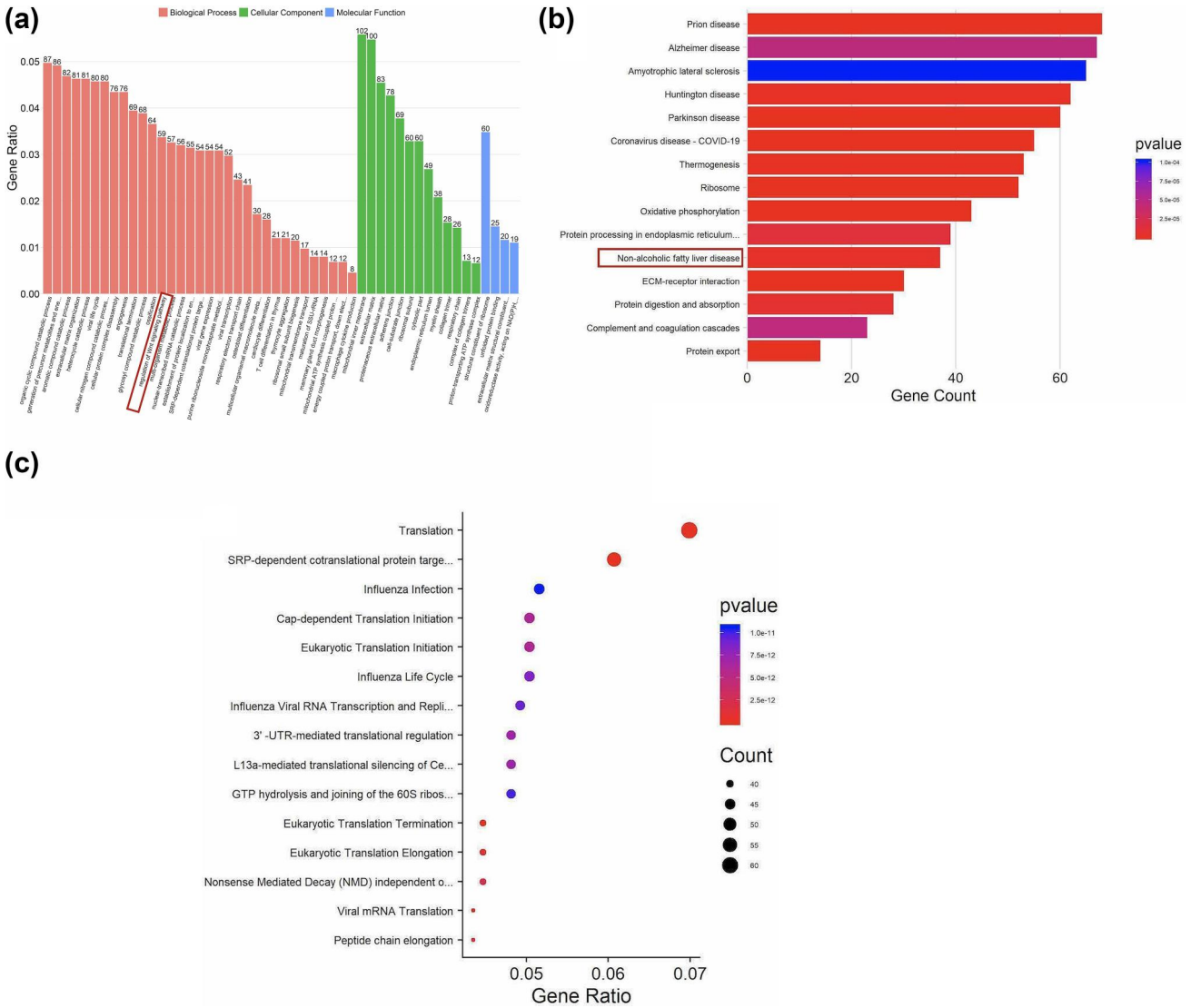

FIGURE 3 GO, KEGG, and Reactome enrichment analysis of DEGs. (a) Top 50 GO enrichment bar plot shows most top 50 significant GO Terms. The numbers are the numbers of genes within the list which are annotated to the GO of interest. In Biological Process, there are 57 genes of interest in "regulation of Wnt signaling pathway". (b) KEGG enrichment plots show most top 15 significant KEGG pathway including 37 genes of interest in "non-alcoholic fatty liver disease". (c) Reactome pathway bubble plot shows most top 15 significant Reactome pathway. Axes show number of gene counts in each process category

Reactome. Most of the pathways identified in Reactome were associated with Translation processes as shown in Figure 3c. However, β-catenin independent Wnt signaling (Path ID 2858494) and Signaling by Wnt (Path ID 195721) were identified as common shared pathways with GO analysis. The full list of the Reactome Pathway enrichment analysis data is provided in Table S6.

Taken together, these results outlined metabolic processes as the hallmark of NAFLD/NASH disease progression and identified Wnt-signaling as a candidate shared for biological pathway-associated with NAFLD/NASH.

Validation of Wnt signaling in NAFLD/NASH using RT^2 profile PCR array and immunoblotting

Based on the biological pathway results, we hypothesized that the observed and documented sexual dimorphism in NAFLD/NASH could be a result of perturbation in Wnt signaling pathway. Wnt signaling was shown to be associated with chronic metabolic diseases and NAFLD-associated hepatocarcinogenesis.[27,28] To test this hypothesis, we used the pathway-focused "Wnt signaling targets" PCR array that allowed to profile the expression of 84 key genes responsive to Wnt signaling. Two NAFLD/NASH samples for each sex (for male: case 14 and 14.1; for female: case 16 and 16.1) were used against two normal samples of the same sex (for male: case 13 and 13.1; for female: case 15 and 15.1). We detected 77 genes overexpressed in female cases and 7 downregulated genes, as shown in Figures 4a,b. Among overexpressed genes in female cases are *WIF1* (Wnt inhibitory factor 1; 814 630-fold), *WNT2* (Wingless-type MMTV integration site family member 2; 18-fold), *LRP6* (Low density lipoprotein receptor-related protein 6; 5-fold), *GSK38* (Glycogen synthase kinase 3 beta; 6-fold), *DVL2* (Disheveled, dsh homolog 2; 23-fold) and *CTNNB1* (β-catenin; 5.9-fold). Among downregulated Wnt-signaling associated genes in NAFLD/NASH female cases are *PITX2* (Paired-like homeodomain 2; 60-fold), *FGF4* (Fibroblast growth factor 4; 98-fold) and *MMP7* (Matrix metallopeptidase 7; 14-fold). Detailed information on these genes is presented in Table 1.

For male cases, we detected 74 overexpressed genes and 10 downregulated, as shown in Figures 4c,d. The most overexpressed genes are *PITX2* (Paired-like homeodomain 2; 15 420-fold), *FZD5* (Frizzled family receptor 5; 11-fold), *PPARD* (Peroxisome proliferator-activated receptor delta; 7-fold), *RHOA* (Ras's homolog gene family, member A; 7-fold), *MTFP1* (Mitochondrial fission process 1; 10-fold) and *SKP2* (S-phase kinase-associated protein 2; 12-fold). Among downregulated Wnt-signaling associated genes in NAFLD/NASH male cases are *WIF1* (Wnt inhibitory factor 1; 39-fold), *WNT6* (Wingless-type MMTV integration site family member 2; 51-fold), *WNT8A* (Wingless-type MMTV integration site family member 8A; 18-fold), *SFRP4* (Secreted frizzled-related protein 4; 10-fold), *LEF1* (Lymphoid enhancer-binding factor 1; 19-fold) and *CCND2* (Cyclin D2; 6-fold). Detailed information on these genes is shown in Table 2. Collectively, these results indicate that perturbation of WNT signaling pathway could be associated with the observed the sexual dimorphism in NAFLD/NASH cases as genes involved in canonical pathway (Wnt/β-catenin activation) such as *CTNNB1*, *Myc* and *CCND2* are overexpressed in female cases, whereas these genes are either not detected or downregulated in male cases (Wnt/β-catenin inactivation).

The expression of selected genes involved in canonical WNT/β-catenin pathway (*CTNNB1*, *WIF1*, *FRZB* and *PITX2*) were further validated with immunoblotting using an independent set of eight tissue samples for both sexes. As shown in Figure 4e, the expression level of β-catenin increased in NASH2 samples (female) as compared to NASH1 (male), which is in concordance with the results obtained with PCR array in Table 1. In contrast however, the expression levels of WIF1, FRZB and PITX2 proteins in NASH samples were different compared to the mRNA levels seen in Tables 1 and 2. These results indicate that the expression of these three genes at mRNA level do not always correlate with their protein levels, as previously reported by others.[29–31]

DISCUSSION

Non-Alcoholic fatty liver disease (NAFLD) remains a major cause of chronic liver disease worldwide. Recently, it has been shown that sexual dimorphism plays a major role in the prevalence, pathogenesis, and progression of NAFLD.[10–13] However, the exact molecular mechanisms for the observed gender disparities that exist in NAFLD are not well understood. Therefore, to better understand the molecular mechanisms and possible signaling pathways associated with NAFLD/NASH gender differences, we performed whole RNA seq on liver tissue samples to identify DEGs between sexes that could be linked to sexual dimorphism, coupled with pathway focused PCR array to validate the expression of functionally related genes associated with Wnt signaling pathway. Immunoblot analysis was also used to validate the expression of specific target proteins associated with Wnt signaling.

In this study, we identified 745 genes that are differentially expressed between female and male cases (FDR q-value < 0.05 and foldchange > 1.5) as presented in Table S3. Interestingly, a significant number of these genes are newly identified with respect to sexual dimorphism in NAFLD, but others had been previously reported to be involved in NAFLD/NASH pathogenesis and progression, such as transcription factors (TFs). Recent studies have indicated that NAFLD is under transcriptional regulation of many TFs. The development of NAFLD and NASH strongly correlates with the dysregulation of transcriptional regulators that play various role in lipid metabolism, inflammation, metabolic stress, and fibrosis.[32] In this study, we show that some of these TFs are sex specific. For example, *SREBF1*, *(C/EBP)α*, *and ATF5* that are associated with lipid metabolism and metabolic stress in NAFLD, and NASH are shown to be upregulated in female cases compared to males.[33–35] In contrast, we identified other TFs such as *AEBP1* and *TGFβ1/1* are upregulated in male cases compared to females. These TFs are known to be

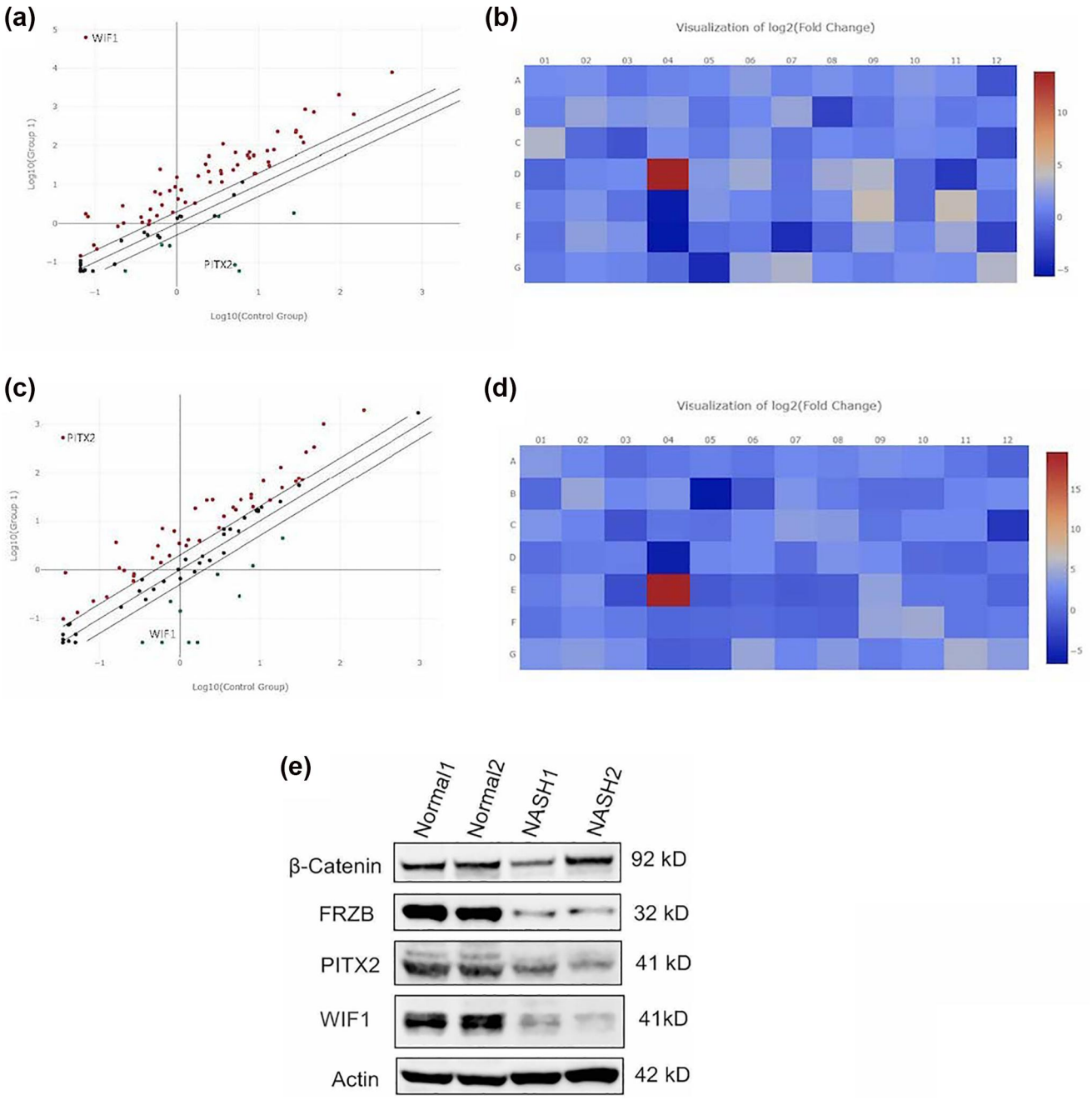

FIGURE 4 DEGs between male and female cases in NAFLD using Wnt focusing RT^2 profiler Polymerase chain reaction (PCR) arrays. (a) Scatter plot comparing the normalized average expression of each gene of the "Wnt targets" PCR array between the two groups (cases 8 & 5 "NAFLD" vs. cases 2 & 3 "normal" in female samples). The red and green dot stand for up-regulated and down-regulated genes, respectively, whereas black dots indicate unchanged genes; cut-off = ±1.5. (b) Visualization of log2 (Fold Change). Two groups of differential genes in female samples, intersect and merge gene expression colorimetry maps. Based on the expression levels of the DEGs in each in groups, a log2 is taken. Using systematic clustering (Hierarchical Cluster), the overall clustering result of the sample is obtained. Red indicates higher expression and blue indicates lower expression. (c) Scatter plot comparing the normalized average expression of each gene of the "Wnt targets" PCR array between the two groups (cases 6 & 7 "NAFLD" vs. cases 1 & 4 "normal") in male samples. (d) Visualization of log2 (Fold Change) of gene expression in male samples. (e) Protein expression of β-catenin, FRZB, PITX2 and WIF1 in normal and NASH samples analyzed by immunoblotting. The samples include Normal 1 (male), Normal 2 (female), NASH 1 (male) and NASH 2 (female). Primary antibodies against β-catenin, FRZB, PITX2 and WIF1 were used for detection. β-Actin was used as the loading (reference) control. Each experiment was repeated at least three times

associated with hepatic fibrosis.[36,37] Thus, transcriptional regulation of NAFLD could be one of the main regulators associated with sexual dimorphism in NAFLD and NASH.

To delineate the biological pathways associated with DEGs, we used 3 different platforms: GO, KEGG, and Reactome pathway analysis. As shown in Tables S4–S6, we identified Wnt-signaling as

TABLE 1 The average expression profile of "Wnt targets" in female cases

	AVG delta Ct		2^(−delta Ct)		Fold change	Fold regulation
Gene symbol	Group 1	Control group	Group 1	Control group	Group 1/Control group	Group 1/Control group
APC	−2.72	0.88	6.595544	0.543093	**12.14**	**12.14**
AXIN1	−1.58	0.60	2.990991	0.661142	**4.52**	**4.52**
AXIN2	−0.59	−0.19	1.504604	1.137906	1.32	1.32
BTRC	−4.97	−3.76	31.326478	13.582787	**2.31**	**2.31**
CSNK1A1	−6.91	−5.15	119.854307	35.473897	**3.38**	**3.38**
CTBP1	−4.30	−3.19	19.644595	9.154157	**2.15**	**2.15**
CTNNB1	−5.04	−2.47	32.900923	5.542375	**5.94**	**5.94**
CTNNBIP1	−0.55	1.45	1.460444	0.366777	**3.98**	**3.98**
DAAM1	−5.84	−2.88	57.245723	7.346327	**7.79**	**7.79**
DAB2	−4.30	−1.81	19.647114	3.500992	**5.61**	**5.61**
DKK1	2.19	3.24	0.218997	0.105590	**2.07**	**2.07**
DKK3	1.03	0.77	0.488232	0.587163	0.83	−1.20
DVL1	−2.45	−2.32	5.475847	5.009182	1.09	1.09
DVL2	−0.83	3.70	1.775936	0.077188	**23.01**	**23.01**
EP300	−4.61	−2.29	24.351631	4.906105	**4.96**	**4.96**
FBXW11	−6.10	−2.96	68.546693	7.777673	**8.81**	**8.81**
FGF4	4.08	−2.54	0.058977	5.801458	**0.01**	**−98.37**
FOSL1	1.83	0.60	0.280441	0.658785	**0.43**	**−2.35**
FRAT1	−2.54	0.67	5.797289	0.627929	**9.23**	**9.23**
FRZB	1.86	3.37	0.276363	0.096765	**2.86**	**2.86**
FZD1	−0.63	−0.13	1.543387	1.093783	1.41	1.41
FZD2	3.41	3.91	0.094211	0.066569	1.42	1.42
FZD3	0.24	2.39	0.845923	0.190811	**4.43**	**4.43**
FZD4	−5.63	−2.95	49.422501	7.729071	**6.39**	**6.39**
FZD5	−3.14	0.06	8.836538	0.958198	**9.22**	**9.22**
FZD6	−2.11	−0.05	4.325407	1.035508	**4.18**	**4.18**
FZD7	1.91	0.28	0.265198	0.820945	**0.32**	**−3.10**
FZD8	−1.75	−0.74	3.361129	1.671991	**2.01**	**2.01**
FZD9	3.19	3.91	0.109323	0.066569	1.64	1.64
GSK3B	−5.82	−3.13	56.555189	8.750037	**6.46**	**6.46**
JUN	−3.98	−0.01	15.779081	1.004814	**15.70**	**15.70**
KREMEN1	−1.52	2.19	2.869861	0.218725	**13.12**	**13.12**
LRP5	−3.56	−2.67	11.819085	6.370899	1.86	1.86
LRP6	−7.40	−5.04	168.403198	32.942654	**5.11**	**5.11**
MAPK8	−6.30	−3.95	78.565653	15.445016	**5.09**	**5.09**
MMP7	−0.90	−4.76	1.863859	27.100968	**0.07**	**−14.54**
NFATC1	−0.45	−0.02	1.367637	1.016428	1.35	1.35
NKD1	−0.10	1.40	1.070483	0.378756	**2.83**	**2.83**
NLK	−3.57	−1.83	11.859867	3.561961	**3.33**	**3.33**

(Continues)

TABLE 1 (Continued)

	AVG delta Ct		2^(−delta Ct)		Fold change	Fold regulation
Gene symbol	Group 1	Control group	Group 1	Control group	Group 1/Control group	Group 1/Control group
PITX2	3.56	−2.37	0.085075	5.153656	**0.02**	**−60.58**
PORCN	−1.23	1.07	2.346043	0.476840	**4.92**	**4.92**
PPARD	−2.89	−0.19	7.400843	1.138909	**6.50**	**6.50**
PRICKLE1	0.75	1.32	0.593247	0.401148	1.48	1.48
RHOA	−7.94	−4.85	245.905675	28.871906	**8.52**	**8.52**
RUVBL1	−4.52	−1.79	22.976893	3.464298	**6.63**	**6.63**
SFRP1	0.97	1.18	0.510767	0.440872	1.16	1.16
SFRP4	3.97	3.91	0.063985	0.066569	0.96	−1.04
SOX17	2.77	3.91	0.146816	0.066569	**2.21**	**2.21**
TCF7	−0.67	0.80	1.593362	0.573289	**2.78**	**2.78**
TCF7L1	−2.82	0.28	7.064003	0.820772	**8.61**	**8.61**
VANGL2	4.08	2.09	0.058977	0.235107	**0.25**	**−3.99**
WIF1	−15.94	3.70	62832.410630	0.077130	**814630.59**	**814630.59**
WISP1	−0.61	−1.70	1.528914	3.257182	**0.47**	**−2.13**
WNT1	4.00	3.73	0.062606	0.075364	0.83	−1.20
WNT10A	3.50	2.52	0.088438	0.174745	0.51	−1.98
WNT11	4.08	3.41	0.058977	0.094399	0.62	−1.60
WNT2	−0.59	3.60	1.508043	0.082260	**18.33**	**18.33**
WNT2B	0.08	1.14	0.947627	0.453453	**2.09**	**2.09**
WNT3	−0.96	0.16	1.949264	0.895374	**2.18**	**2.18**
WNT3A	4.08	3.91	0.058977	0.066569	0.89	−1.13
WNT4	1.47	2.25	0.361128	0.210527	1.72	1.72
WNT5A	−0.04	2.16	1.025955	0.224233	**4.58**	**4.58**
WNT5B	−0.23	1.11	1.171940	0.463791	**2.53**	**2.53**
WNT6	4.08	3.91	0.058977	0.066569	0.89	−1.13
WNT7A	3.87	3.91	0.068281	0.066569	1.03	1.03
WNT7B	3.56	3.91	0.084627	0.066569	1.27	1.27
WNT8A	4.08	3.91	0.058977	0.066569	0.89	−1.13
WNT9A	4.08	3.79	0.058977	0.072208	0.82	−1.22
BOD1	−5.76	−1.31	54.156253	2.482743	**21.81**	**21.81**
CALM1	−6.80	−1.88	111.333367	3.690371	**30.17**	**30.17**
CCND1	−4.29	−3.16	19.592552	8.926590	**2.19**	**2.19**
CCND2	−1.82	−0.35	3.522472	1.275956	**2.76**	**2.76**
CHSY1	−4.08	−0.87	16.942152	1.832718	**9.24**	**9.24**
CXADR	−7.86	−4.10	231.852460	17.164705	**13.51**	**13.51**
CYP4V2	−7.80	−4.84	222.408269	28.550516	**7.79**	**7.79**
HSPA12A	−0.65	−1.54	1.572574	2.912349	0.54	−1.85
LEF1	1.20	0.69	0.434667	0.618600	0.70	−1.42
MT1A	−9.76	−5.22	865.818699	37.257724	**23.24**	**23.24**
MTFP1	−3.56	−1.36	11.767780	2.565546	**4.59**	**4.59**

TABLE 1 (Continued)

Gene symbol	AVG delta Ct		2^(−delta Ct)		Fold change	Fold regulation
	Group 1	Control group	Group 1	Control group	Group 1/Control group	Group 1/Control group
MTSS1	−6.07	−2.39	66.970792	5.226073	**12.81**	**12.81**
MYC	−5.28	−3.72	38.914297	13.216519	**2.94**	**2.94**
NAV2	−6.21	−3.68	73.942211	12.811212	**5.77**	**5.77**
PRMT6	−4.66	0.67	25.293671	0.626918	**40.35**	**40.35**
SKP2	−5.08	−1.18	33.905387	2.261829	**14.99**	**14.99**

Note: Group 1 (test group–NASH) = Cases 5 & 8; Control 1 (normal group) = Cases 2 & 3.

a candidate shared by these three platforms. The Wnt signaling pathway, an evolutionary conserved molecular transduction cascade, has been identified to play a major role in various diseases, including chronic liver diseases and NAFLD.[38–40] The Wnt signaling pathway has been classified into the canonical-and non-canonical pathways according to whether the accumulation of β-catenin in the nucleus is necessary or not. The canonical β-catenin pathway is centered on regulating the levels of its major effector β-catenin.[41] In the absence of Wnt ligands, β-catenin is sequestered in the cytoplasm by a protein complex composed of the scaffolding protein Axin, adenomatous polyposis coli (APC) gene product, CK1 and GSK3β. Specific serine and threonine residues in the amino terminal region of β-catenin are sequentially phosphorylated by CK1 and GSK3β. Phosphorylated β-catenin is then ubiquinated and targeted for proteasomal degradation.[42] As a result of this continuous degradation, β-catenin is prevented from accumulating in the cytoplasm, and therefore from reaching the nucleus (inactive canonical pathway). In the absence of nuclear β-catenin, Wnt target genes are repressed by binding of the T-cell factor/lymphoid enhancer factor (TCF/LEF) family of proteins. The canonical pathway is activated when Wnt ligands bind to the transmembrane Frizzled (Fz) receptor and the Fz-coreceptors low density lipoprotein receptor-related protein (LRP) 5 or 6. The complex formed by Wnt-Fz-LRP5/6 is followed by recruitment of the scaffolding protein Disheveled (Dvl), phosphorylation of LRP6 and recruitment of the axin degradation complex. These events prevent phosphorylation of β-catenin and result in its stabilization and cytoplasmic accumulation. β-Catenin then translocated to the nucleus where it forms a complex with the TCF/LEF TFs and activates target gene expression such as *c-myc* and *cyclin D1*.[42]

To confirm the association of Wnt/β-catenin signaling in NAFLD sexual dimorphism based on the biological pathway analysis, we used an RT^2 Profiler PCR array system to analyze the expression of Wnt signaling components (Wnt ligands, receptors, and β-catenin destruction complex) as well as β-catenin targets. Among the 84 genes involved in Wnt signaling pathway, a remarkable expression changes at the mRNA level were observed for several Wnt-related genes as shown in Tables 1 and 2, confirming the inter-relationship of Wnt/β-catenin in the pathogenesis of NAFLD, and hence the reliability of our approach.[39,40] However, the expression level of these transcripts is different between female and male cases. For example, transcripts that are associated with active components of Wnt signaling such as *APC*, *AXIN1*, *Dvl2*, *GSK3β*, *LRP6*, *TCF7L1*, and *CTNNB1* are highly expressed in female specific NAFLD cases (Table 1) and either repressed or not expressed in male specific NAFLD cases (Table 2). Of the activated Wnt targets, four transcripts: *JUN* (Jun proto-oncogene, AP-1 transcription factor subunit), *PPARD*, *CCND1*, and *MYC* are significantly upregulated in female cases (Table 1). Other Wnt targets such as *MMP7* and *LEF1* are repressed in male cases (Table 2). A comprehensive updated list of Wnt targets can be found at http://www.stanford.edu/group/nusselab/cgi-bin/wnt/target_genes. These data of particular interest as they may suggest, for the first time, that the activation of canonical Wnt signaling could be one of the main pathways associated with sexual dimorphism in NAFLD and NASH. Further studies using larger sample size could help to clarify the present findings, as these results suggest that Wnt signaling components and targets may have important role in sex-based pathogenesis of NAFLD/NASH and may facilitate sex specific therapy of NAFLD.

Strong differential regulation in Wnt signaling was detected for the transcription factor *PITX2* (>60 fold down regulation) in female NAFLD cases (Table 1; Figures 4a,b); whereas in male NAFLD cases it is drastically up regulated (>15 000 fold) as shown in Table 2 and Figures 4c,d. *PITX2* represent a direct target gene of Wnt/β-catenin signaling was shown to be expressed in several tissues that are developmentally regulated by Wnt/β-catenin signaling such as kidney, pituitary and liver.[43–45] *PITX2* acts as a downstream effector of developmental regulatory pathways and has been shown to interact with both canonical and no-canonical Wnt pathways.[41] The exact mechanism for the observed sex-based differential expression of *PITX2* in our study is not well understood but it is conceivably possible related to the expression of *PITX2* isoforms and corresponding mRNAs stability.[46] In fact, previous studies have shown that *PITX2* isoforms are involved in sexual dimorphism of gonads in rat.[47] Thus, further study is needed to investigate further the role of PITX2 isoforms in sexual dimorphism of NAFLD. *WIF1* was also found to be differentially expressed in a sexually dimorphic manner. *WIF1* is a member of secreted upstream antagonists of the Wnt signaling pathway. These antagonists can be divided into two functional classes: the SFRP class and the Dickkopf class. Members of the SFRP class, which include the SFRP (secreted Frizzled-related

TABLE 2 The average expression profile of "Wnt targets" in male cases

	AVG delta Ct		2^(−delta Ct)		Fold change	Fold regulation
Gene symbol	Group 1	Control group	Group 1	Control group	Group 1/Control group	Group 1/Control group
APC	−0.49	0.79	1.405003	0.578243	**2.43**	**2.43**
AXIN1	−0.96	0.43	1.944976	0.740381	**2.63**	**2.63**
AXIN2	−0.03	0.07	1.022706	0.951642	1.07	1.07
BTRC	−4.08	−3.26	16.857882	9.576026	1.76	1.76
CSNK1A1	−6.15	−5.08	70.970081	33.877698	**2.09**	**2.09**
CTBP1	−4.25	−2.20	19.050542	4.593144	**4.15**	**4.15**
CTNNB1	−3.53	−2.69	11.568431	6.468037	1.79	1.79
CTNNBIP1	0.42	1.91	0.749381	0.265736	**2.82**	**2.82**
DAAM1	−4.02	−3.20	16.205410	9.160594	1.77	1.77
DAB2	−3.65	−1.82	12.526374	3.528105	**3.55**	**3.55**
DKK1	2.91	4.27	0.133422	0.051865	**2.57**	**2.57**
DKK3	0.31	−1.55	0.806252	2.934941	**0.27**	**−3.64**
DVL1	−2.42	−1.82	5.367755	3.519465	1.53	1.53
DVL2	−0.13	2.51	1.094076	0.175716	**6.23**	**6.23**
EP300	−4.09	−2.31	17.066546	4.956135	**3.44**	**3.44**
FBXW11	−5.13	−2.97	34.981046	7.854214	**4.45**	**4.45**
FGF4	4.95	4.87	0.032368	0.034276	0.94	−1.06
FOSL1	1.85	3.03	0.277467	0.122406	**2.27**	**2.27**
FRAT1	−1.64	0.91	3.107617	0.532921	**5.83**	**5.83**
FRZB	2.81	−0.01	0.142361	1.007954	**0.14**	**−7.08**
FZD1	−0.93	−0.93	1.899912	1.906587	1.00	−1.00
FZD2	3.34	4.85	0.098709	0.034565	**2.86**	**2.86**
FZD3	1.45	1.68	0.366353	0.312292	1.17	1.17
FZD4	−3.99	−3.26	15.881787	9.551219	1.66	1.66
FZD5	−2.81	0.72	7.024515	0.605274	**11.61**	**11.61**
FZD6	−0.64	−1.23	1.560267	2.348861	0.66	−1.51
FZD7	2.16	0.39	0.223802	0.761783	**0.29**	**−3.40**
FZD8	−1.65	−0.26	3.139401	1.196164	**2.62**	**2.62**
FZD9	4.41	4.87	0.047126	0.034276	1.37	1.37
GSK3B	−4.90	−2.97	29.851752	7.838788	**3.81**	**3.81**
JUN	−0.46	−0.82	1.373701	1.759550	0.78	−1.28
KREMEN1	0.76	1.93	0.591133	0.263259	**2.25**	**2.25**
LRP5	−2.77	−2.08	6.811091	4.221693	1.61	1.61
LRP6	−6.25	−4.94	76.368679	30.657122	**2.49**	**2.49**
MAPK8	−4.75	−3.75	26.921880	13.456735	**2.00**	**2.00**
MMP7	−2.15	−4.27	4.450274	19.303545	**0.23**	**−4.34**
NFATC1	0.14	−0.61	0.908486	1.525501	0.60	−1.68
NKD1	0.67	1.57	0.628982	0.337673	1.86	1.86
NLK	−2.86	−1.62	7.284585	3.072387	**2.37**	**2.37**
PITX2	−9.05	4.87	528.543637	0.034276	**15420.07**	**15420.07**

TABLE 2 (Continued)

	AVG delta Ct		2^(−delta Ct)		Fold change	Fold regulation
Gene symbol	Group 1	Control group	Group 1	Control group	Group 1/Control group	Group 1/Control group
PORCN	−0.82	1.14	1.760506	0.454959	**3.87**	**3.87**
PPARD	−2.64	0.24	6.222740	0.849425	**7.33**	**7.33**
PRICKLE1	0.79	0.67	0.576892	0.628875	0.92	−1.09
RHOA	−8.05	−5.24	265.875678	37.889338	**7.02**	**7.02**
RUVBL1	−4.19	−0.63	18.287076	1.549564	**11.80**	**11.80**
SFRP1	2.03	1.42	0.245287	0.374820	0.65	−1.53
SFRP4	4.95	1.55	0.032368	0.340558	**0.10**	**−10.52**
SOX17	3.75	4.64	0.074579	0.040080	1.86	1.86
TCF7	−0.70	−0.24	1.627612	1.178791	1.38	1.38
TCF7L1	−2.04	−0.34	4.122280	1.270040	**3.25**	**3.25**
VANGL2	2.53	2.43	0.172702	0.185040	0.93	−1.07
WIF1	4.95	−0.36	0.032368	1.287651	**0.03**	**−39.78**
WISP1	−1.80	0.03	3.473039	0.979781	**3.54**	**3.54**
WNT1	3.68	4.58	0.077819	0.041712	1.87	1.87
WNT10A	4.40	4.33	0.047475	0.049650	0.96	−1.05
WNT11	2.13	3.58	0.228557	0.083403	**2.74**	**2.74**
WNT2	0.20	4.76	0.871866	0.036827	**23.67**	**23.67**
WNT2B	0.60	−0.02	0.659783	1.011502	0.65	−1.53
WNT3	−1.87	2.64	3.652491	0.160248	**22.79**	**22.79**
WNT3A	4.95	4.87	0.032368	0.034276	0.94	−1.06
WNT4	1.33	1.09	0.398376	0.470233	0.85	−1.18
WNT5A	0.04	2.31	0.971509	0.201739	**4.82**	**4.82**
WNT5B	0.29	1.90	0.817716	0.267281	**3.06**	**3.06**
WNT6	4.95	−0.73	0.032368	1.655163	**0.02**	**−51.14**
WNT7A	4.86	4.62	0.034424	0.040544	0.85	−1.18
WNT7B	4.74	4.87	0.037530	0.034276	1.09	1.09
WNT8A	4.95	0.74	0.032368	0.596985	**0.05**	**−18.44**
WNT9A	4.95	4.35	0.032368	0.049039	0.66	−1.52
BOD1	−4.78	−2.53	27.508174	5.776895	**4.76**	**4.76**
CALM1	−4.26	−3.40	19.193225	10.579315	1.81	1.81
CCND1	−7.01	−4.20	128.853243	18.365812	**7.02**	**7.02**
CCND2	−0.28	−3.05	1.210238	8.254661	**0.15**	**−6.82**
CHSY1	−2.64	−2.43	6.212863	5.393501	1.15	1.15
CXADR	−6.04	−4.82	65.813622	28.330882	**2.32**	**2.32**
CYP4V2	−5.76	−4.95	54.230720	30.971030	1.75	1.75
HSPA12A	−1.15	−1.81	2.213572	3.502004	0.63	−1.58
LEF1	1.80	−2.47	0.288160	5.532519	**0.05**	**−19.20**
MT1A	−6.08	−3.48	67.675032	11.133764	**6.08**	**6.08**
MTFP1	−4.78	−1.35	27.502647	2.547943	**10.79**	**10.79**

(Continues)

TABLE 2 (Continued)

Gene symbol	AVG delta Ct		2^(−delta Ct)		Fold change	Fold regulation
	Group 1	Control group	Group 1	Control group	Group 1/Control group	Group 1/Control group
MTSS1	−4.30	−3.05	19.647591	8.277944	**2.37**	**2.37**
MYC	−4.65	−4.17	25.067326	18.053751	1.39	1.39
NAV2	−5.61	−4.25	48.717902	18.987070	**2.57**	**2.57**
PRMT6	−1.98	−0.81	3.953818	1.753618	**2.25**	**2.25**
SKP2	−4.75	−1.11	26.953470	2.158679	**12.49**	**12.49**

Note: Group 1 (test group–NASH) = Cases 6 & 7; Control 1 (normal group) = Cases 1 & 4.

protein) family like WIF1 (Wnt inhibitory factor 1) directly bind to Wnt proteins and thereby prevent their activating the Wnt pathway. Members of Dickkopf class antagonize Wnt signaling by direct interaction with the Wnt receptor complex.[48] *WIF1* was found to be drastically upregulated (>800 000 fold) in female NAFLD cases (Table 1; Figures 4a,b); whereas in male NAFLD cases it is drastically down regulated (39-fold) as shown in Table 2 and Figures 4c,d. Interesting, *WIF1* was found to be down-regulated in several cancer types, like prostate, breast and lung cancer but upregulated in Wilms tumors.[49] This overexpression may be a negative feedback mechanisms in tumors with uncontrolled Wnt signaling.[50] It will be of interest in the future to analyze larger cohorts to determine the biological role of *WIF1* in NAFLD sexual dimorphism. Surprisingly, we were unable to validate protein expression of many genes that correlated with Wnt-associated mRNA like *PITX2* and *WIF1* as it is well accepted that mRNA levels do not always reflect protein levels because of downstream translational control mechanisms as shown by others.[30,31]

Our study has several limitations. One of the limitations of the current study was the use of whole liver tissues comprised of multiple cell types; such cellular complexity compromises the detection of genes expressed in cell subsets of liver tissues. Although the present study was limited by the relatively small number of available human liver tissues samples, the data show a clear and robust distinction between female and male cases with respect gene expression in NAFLD/NASH compared to normal. Our conclusions are based solely on analysis of gene expression profiles, the exact effects of identified genes in involved in sexual dimorphisms like *PITX2* and *WIF1* need to be further confirmed by additional biological experiments. Future validation experiments using large sample size are thus warranted to examine these results.

In summary, the research presented here provides, for the first time, preliminary evidence for potential molecular mechanisms underlying the observed sexual dimorphism in NAFLD/NASH progression. Using multi-omics approach, we identified differentially expressed transcripts that are sex specific, and many associated with dysregulation of Wnt/β-Catenin signaling pathway. The most activated Wnt pathway related genes, like *PITX2* and *WIF1* may have potential as predictive biomarkers and targeted therapeutics for NAFLD/NASH sex-based clinical approach.

ACKNOWLEGMENTS

The human liver specimens were obtained through the Liver Tissue Cell Distribution System (Minneapolis, MN), which is funded by the National Institute of Health Contract No. N01-DK-7-0004/HHSN267200700004C. This work was supported by CPPS-WSU (17A-2957-9838) to SD.

CONFLICT OF INTERESTS

The authors declare that they have no conflict of interest.

ETHICS STATEMENTS

Washington State University (WSU) Office of Research Assurances has found that the study is exempt from the need for the Institutional Research Board (IRB) approval. Twenty-four snapped frozen tissue samples were obtained from the IRB approved University of Minnesota, Liver Tissue Cell Distribution System (Minneapolis, MN). All specimens with anonymized identifiers were histopathological confirmed by a pathologist.

DATA AVAILABILITY STATEMENT

The data that support the findings of this study are available from the corresponding author upon reasonable request.

ORCID

Matthew M Yeh https://orcid.org/0000-0002-3004-8799
Xiuhui Shi https://orcid.org/0000-0002-5327-8247
Jingxuan Yang https://orcid.org/0000-0003-3265-161X
Min Li https://orcid.org/0000-0002-3971-9130
Kar-Ming Fung https://orcid.org/0000-0002-4623-9469
Sayed S. Daoud https://orcid.org/0000-0003-0757-8166

REFERENCES

1. Younossi Z, Anstee QM, Marietti M, Hardy T, Henry L, Eslam M, et al. Global burden of NAFLD and NASH: trends, predictions, risk factors and prevention. Nat Rev Gastroenterol Hepatol. 2018; 15(10):11–20.
2. Chalasani N, Younossi Z, Lavine JE, Charlton M, Cusi K, Rinella M, et al. The diagnosis and management of nonalcoholic fatty liver disease: practice guidance from the American association for the study of liver diseases. Hepatology. 2018;67(1):328–57.
3. Araujo AR, Rosso N, Bedogni G, Tiribelli C, Bellentani S. Global epidemiology of non-alcoholic fatty liver disease/non-alcoholic

steatohepatitis: what we are need in the future. Liver Int. 2017;38:47–51.
4. Koch LK, Yeh MM. Nonalcoholic fatty liver disease (NAFLD): diagnosis, pitfalls, and staging. Ann Diagn Pathol. 2018;37:83–90.
5. Romeo S, Kozlitina J, Xing C, Pertsemlidis A, Cox D, Pennacchio LA, et al. Genetic variation in PNPLA3 confers susceptibility to nonalcoholic fatty liver disease. Nat Genet. 2008;40:1461–5.
6. Singal AG, Manjunath H, Yopp AC, Beg MS, Marrero JA, Gopal P, et al. The effect of PNPLA3 on fibrosis progression and development of hepatocellular carcinoma: a meta-analysis. Am J Gastroenterol. 2014;109(3):325–34.
7. Kozlitina J, Smagris E, Stender S, Nordestgaard BG, Zhu HH, Tybjaerg-Hansen A, et al. Exome-wide association study identifies TM6SF2 variant that confers susceptibility to nonalcoholic fatty liver disease. Nat Genet. 2014;46:352–6.
8. Mancina RM, Dongiovanni P, Petta S, Pingitore P, Meroni M, Rametta R, et al. The MBOAT7-TMC4 variant rs641738 increases risk of nonalcoholic fatty liver disease in individuals of European descent. Gastroenterology. 2016;150(5):1219–30.
9. Petta S, Miele L, Bugianesi E, Camma C, Rosso C, Boccia S, et al. Glucokinase regulatory protein gene polymorphism affects liver fibrosis in nonalcoholic fatty liver disease. PLoS One. 2014;9(2):1–7.
10. Salvoza NC, Giraudi PJ, Tiribelli C, Rosso N. Sex differences in non-alcoholic fatty liver disease: hints for future management of the disease. Explor Med. 2020;1:51–74.
11. Lonardo A, Nascimbeni F, Ballestri S, Fairweather D, Win S, Than TA, et al. Sex differences in NAFLD: state of the art and identification of research gap. Hepatology. 2019;70(4):1457–69.
12. DiStefano JK. NAFLD and NASH in postmenopausal women: implications for diagnosis and treatment. Endocrinology. 2020;161(10):1–12.
13. Balakrishnan M, Patel P, Dunn-Valadez S, Dao C, Khan V, Ali H, et al. Women have a lower risk of nonalcoholic fatty liver disease but a higher risk of progression vs men: a systematic review and meta-analysis. Clin Gastroenterol Hepatol. 2021;19:61–71.
14. Langmead B, Salzberg SL. Fast gapped-read alignment with Bowtie. Nat Methods. 2012;9(4):357–9.
15. Li B, Dewey CN. RSEM: accurate transcript quantification from RNA-Seq data with or without a reference genome. BMC Bioinf. 2011;12:323–39.
16. Robinson MD, McCarthy DJ, Smyth GK. edgeR: a Bioconductor package for differential expression analysis of digital gene expression data. Bioinformatics. 2010;26(1):139–40.
17. Young MD, Wakefield MJ, Smyth GK, Oshlack AL. Gene ontology analysis for RN-seq: accounting for selection bias. Genome Biol. 2010;11(2):R14–26.
18. Xie C, Mao X, Huang J, Ding Y, Wu J, Dong S, et al. KOBAS 2.0: a web server for annotation and identification of enriched pathways and diseases. Nucleic Acids Res. 2011;39:W316–22.
19. Kanehisa M, Araki M, Goto S, Hattori M, Hirakawa M, Itoh M, et al. KEGG for linking genomes to life and the environment. Nucleic Acids Res. 2008;36:D480–4.
20. Draghici S, Khatri P, Tarca AL, Amin K, Done A, Voichita C, et al. A systems biology approach for pathway level analysis. Genome Res. 2007;17:1537–45.
21. Livak KJ, Schmittgen TD. Analysis of relative gene expression data using real-time quantitative PCR and the 2(-Delta Delta C(T)) method. Methods. 2001;25:402–8.
22. Shi L, Reid LH, Jones WD, Shippy R, Warrington JA, Baker SC, et al. The MicroArray Quality Control (MAQC) project shows inter- and intraplatform reproducibility of gene expression measurements. Nat Biotechnol. 2006;24:1151–61.
23. Shi L, Campbell G, Jones WD, Campagne F, Wen Z, Walker SJ, et al. The MicroArray Quality Control (MAQC)-II study of common practices for the development and validation of microarray-based predictive models. Nat Biotechnol. 2010;28:827–38.
24. Rehman A, Chahal MS, Tang X, Bruce JE, Pommier Y, Daoud SS. Proteomic identification of heat shock protein 90 as a candidate target for p53 mutation reactivation by PRIMA-1 in breast cancer cells. Breast Cancer Res. 2005;7(5):R765–75.
25. Suppli MP, Rigbolt KTG, Veidal SS, Heeboll S, Eriksen PL, Demant M, et al. Hepatic transcriptome signatures in patients with varying degree of nonalcoholic liver disease compared with healthy normal-weight individuals. Am J Physiol Gastrointest Liver Physiol. 2019;316:G462–72.
26. Bruschi FV, Tardelli M, Herac M, Claudel T, Trauner M. Metabolic regulation of hepatic PNPLA3 expression and severity of liver fibrosis in patients with NASH. Liver Int. 2020;40(5):1098–110.
27. Wang S, Song K, Srivastava R, Dong C, Go GW, Li N, et al. Nonalcoholic fatty liver disease induced by noncanonical Wnt and its rescue by Wnt3a. Faseb J. 2015;29(8):3436–45.
28. Tian Y, Mok MT, Yang P, Cheng ASL. Epigenetic activation of Wnt/B-catenin signaling in NAFLD-associated hepatocarcinogenesis. Cancers. 2016;8:76–7.
29. Leijten JC, Bos SD, Landman EB, Georgi N, Jahr H, Meulenbelt I, et al. GREM1, FRZB and DKK1 mRNA levels correlate with osteoarthritis-associated factors. Arthritis Rs Ther. 2013;15:R126.
30. Fung FK, Chan DW, Liu VW, Leung TH, Cheung AN, Ngan HY. Increased expression of PITX2 transcription factor contributes to ovarian cancer progression. PLoS. 2012;7(5):e7076.
31. Song G, Cao HX, Yao SX, Li C-T. Abnormal expression of WIF1 in hepatocellular carcinoma cells and its regulating effect on invasion and metastasis factors TIMP-3 and caveolin-1 of hepatocellular carcinoma. Asian Pacific J Trop Med. 2015;8(11):958–63.
32. Steensels S, Qiao J, Ersoy BA. Transcriptional regulation in non-alcoholic fatty liver disease. Metabolites. 2020;10:283–316.
33. Zhao X-Y, Xiomg X, Liu T, Mi L, Peng X, Rui C, et al. Long noncoding RNA licensing of obesity-linked hepatic lipogenesis and NAFLD pathogenesis. Nat Commun. 2018;9(1):2986–3000.
34. Lake AD, Chaput AL, Novak P, Cherrington NJ, Smith CL. Transcription factor binding site enrichment analysis predicts drivers of altered gene expression in non-alcoholic steatohepatitis. Biochem Pharmacol. 2016;122:62–71.
35. Lee S, Kim S, Hwang S, Cherrington NJ, Ryu D-Y. Dysregulated expression of proteins associated with ER stress, autophagy, and apoptosis in tissues from non-alcoholic fatty liver disease. Oncotarget. 2017;8:63370–81.
36. Gerhard G, Hanson A, Wilhelmsem D, Piras I, Still CD, Chu X, et al. AEBP1 expression increases with severity of fibrosis in NASH and is regulated by glucose, palmitate, and mIR-372-3p. PLoS One. 2019;14(7):e0219764.
37. Kyritsi K, Francis H, Zhou T, Ceci L, Wu N, Yang Z, et al. Down-regulation of p16 decreases biliary damage and liver fibrosis in the Mdr2/mouse model of primary sclerosing cholangitis. Gene Expr. 2020;20(2):89–103.
38. Nusse R, Clevers H. Wnt/β-catenin signaling, disease, and emerging therapeutic modalities. Cell. 2017;169(6):985–99.
39. Ackers I, Malgor R. Interrelationship of canonical and non-canonical Wnt-signaling pathways in chronic metabolic diseases. Diabetes Vasc Dis Res. 2018;15(1):3–13.
40. Wang X-M, Wang X-Y, Huang Y-M, Chen X, Lu MH, Shi L, et al. Role and mechanisms of action of microRNA-21 as regards the regulation of the Wnt/β-catenin signaling pathway in the pathogenesis of non-alcoholic fatty liver disease. Int J Mol Med. 2019;44:2201–12.
41. Gordon MD, Nusse R. Wnt signaling multiple pathways, multiple receptors, and multiple transcription factors. J Biol Chem. 2006;281(32):22429–33.

42. Thompson MD, Monga SPS. Wnt/β-Catenin signaling in liver health and disease. Hepatology. 2007;45(5):1298–305.
43. Schubert SW, Kardash E, Khan MA, Cheusova T, Kilian K, Wegner M, et al. Interaction, cooperative promoter modulation, and renal colocalization of GCMa and PITX2. J Biol Chem. 2004;279(48): 50358–65.
44. Kioussi C, Briata P, Baek SH, Rose DW, Hamblet NS, Herman T, et al. Identification of a Wnt/Dvl/beta-Catenin/Pitx2 pathway mediating cell type specific proliferation during development. Cell. 2002;111: 673–85.
45. Jochheim-Richter A, Rudrich U, Koczan D, Hillemann T, Tewes S, Petry M, et al. Gene expression analysis identifies novel genes participating in early murine liver development and adult liver regeneration. Differentiation. 2006;74(4):167–73.
46. Cox CJ, Espinoza HM, McWilliams B, Hjalt TA, Semina EV, Amendt BA, et al. Differential regulation of gene expression by PTX2 isoforms. J Biol Chem. 2002;277(28):25001–10.
47. Nandi SS, Ghosh P, Roy SS. Expression of PITX2 homeodomain transcription factor during rat gonadal development in a sexually dimorphic manner. Cell Physiol Biochem. 2011;27(2):159–70.
48. Kawano Y, Kypta R. Secreted antagonists of the Wnt signaling pathway. J Cell Sci. 2003;116:2627–34.
49. Wissmann C, Wild PJ, Kaiser S, Roepcke S, Stoehr R, Woenckhaus M, et al. WIF1, a component of the Wnt pathway, is downregulated in prostate, breast, lung, and bladder cancer. J Pathol. 2003; 201:204–12.
50. Zirn B, Samans B, Wittmann S, Pietsch T, Leuschner I, Graf N, et al. Target genes of the Wnt/beta Catenin pathway in Wilms tumors. Genes Chromosomes Cancer. 2006;45(6):565–74.

SUPPORTING INFORMATION

Additional supporting information may be found in the online version of the article at the publisher's website.

How to cite this article: Yeh MM, Shi X, Yang J, Li M, Fung K-M, Daoud SS. Perturbation of Wnt/β-catenin signaling and sexual dimorphism in non-alcoholic fatty liver disease. Hepatol Res. 2022;52(5):433–48. https://doi.org/10.1111/hepr.13754